University of Amsterdam

UvA-DARE (Digital Academic Repository)

Phase transition to bundles of flexible supramolecular polymers

Huisman, B.A.H.; Bolhuis, P.G.; Fasolino, A.

[Link to publication](#)

Phase Transition to Bundles of Flexible Supramolecular Polymers

B. A. H. Huisman, P. G. Bolhuis, and A. Fasolino

Van 't Hoff Institute for Molecular Sciences, University of Amsterdam, Nieuwe Achtergracht 166,
1018 WV Amsterdam, The Netherlands
(Received 1 November 2007; published 5 May 2008)

We report Monte Carlo simulations of the self-assembly of supramolecular polymers based on a model of patchy particles. We find a first-order phase transition, characterized by hysteresis and nucleation, toward a solid bundle of polymers, of length much greater than the average gas phase length. We argue that the bundling transition is the supramolecular equivalent of the sublimation transition, which results from a weak chain-chain interaction. We provide a qualitative equation of state that gives physical insight beyond the specific values of the parameters used in our simulations.

Self-assembly is an active field of research, driven by the desire to design new materials. Understanding the rules of self-assembly has been defined as the challenge of this century for chemistry [1]. The large molecules involved in self-assembly spontaneously organize because of highly specific interactions such as hydrophobic or hydrophilic, hydrogen bonding, and π-π stacking. Modeling these self-assembly processes using coarse-grained models, such as the patchy particle [2], has the potential to yield theoretical insight. Up to now, patchy-particle models have mostly been used to describe the self-assembly of functionalized colloids for photonic crystals [3] and to study the formation of self-assembled clusters [4].

We focus on linear supramolecular self-organization, such as the experimentally observed reversible aggregation of discotic molecules into supramolecular polymers [5–7]. Sciortino *et al.* [2] showed that the Wertheim thermodynamic perturbation theory (WTPT) of associating liquids accurately predicts the chain-length distribution by comparing the WTPT to simulations of square-well patchy particles. One step beyond linear polymerization is the bundling of supramolecular chains [5–7] that neither the WTPT nor the square-well patchy particle can deal with, since it requires chain-chain interactions.

In this Letter we present Monte Carlo simulations of patchy particles that, by decreasing temperature or increasing density first polymerize into chains and subsequently undergo a phase transition toward bundles of these chains. We interpret this bundling as a sublimation transition from a polymer gas to a solid bundle. This sublimation competes with polymerization and gives rise to nontrivial phase behavior. We propose a simple thermodynamic model to describe the transition.

Our coarse-grained model of disklike molecules consists of hard spheres of diameter σ, dressed by two opposing patches. The orientation-dependent patch potential not only allows chain formation but also exhibits a weak chain-chain interaction. The potential between patch i directed along the vector $\vec{p}_i$ and patch j along $\vec{p}_j$, illustrated in Fig. 1, is given by a Lennard-Jones potential of the

interparticle distance $r = |\vec{r}_{ij}|$ modulated by three directional components

$$V(r, \theta_i, \theta_j, \theta_{ij}) = 4\epsilon\left[\left(\frac{\sigma}{r}\right)^{12} - \left(\frac{\sigma}{r}\right)^6\right]$$
$$\times \exp\left[-\frac{\theta_i^2 + \theta_j^2 + \theta_{ij}^2}{4w^2}\right], \quad (1)$$

where ϵ is the maximum energy of interaction and w penalizes nonperfect alignment. We truncate $V(r)$ of Eq. (1) at $r_c = 2.3\sigma$ and shift and rescale it to have $V(r_c) = 0$ and $V(2^{1/6}\sigma) = -\epsilon$. The first two directional components favor minimization of the angle θ_i between the patch direction $\vec{p}_i$ of patch i and the interparticle vector
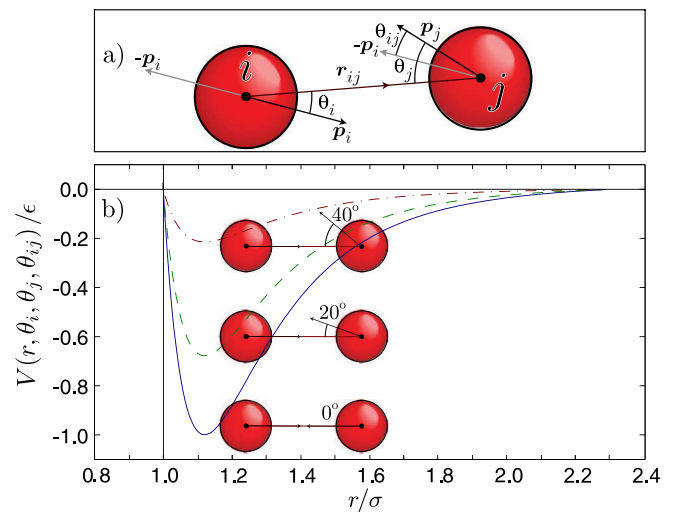
FIG. 1 (color online). (a) Geometry of the patches. θ_i is the angle between the direction $\vec{p}_i$ of patch i and the interparticle vector $\vec{r}_{ij} = \vec{r}_j - \vec{r}_i$. θ_j is the angle between the direction $\vec{p}_j$ of patch j and $\vec{r}_{ji} = -\vec{r}_{ij}$. θ_{ij} is the angle between $\vec{p}_j$ and $-\vec{p}_i$. (b) Patch potential for three values of θ_j for $w = 0.4$. The strongest attraction occurs for $\theta_i = \theta_j = \theta_{ij} = 0$ and decreases rapidly for increasing angles. Particles are depicted at half their size.

$\vec{r}_{ij}$, and of the angle θ_j between $\vec{p}_j$ and $\vec{r}_{ji} = -\vec{r}_{ij}$. The third component minimizes the angle θ_{ij} between $\vec{p}_j$ and $-\vec{p}_i$, favoring parallel alignment of the patches. This potential has three advantages compared to a square-well patch potential [2]. First, it allows multiple bonds without increasing the energy per interaction site in discrete steps. This feature introduces a slight interaction between molecules in neighboring chains. Second, the desired parallel alignment of neighboring patches prevents branching (and therefore network formation) of the polymers. Finally, it allows us to tune the flexibility of a supramolecular chain. One can show that w is a measure of the chain flexibility by calculating the bending rigidity κ, and hence the persistence length l_p of a chain [8]

$$E_{\text{bend}} = \frac{\kappa}{2} \int_0^L \frac{1}{R(s)^2} ds \Rightarrow \kappa = 2^{1/6} \frac{3\sigma\epsilon}{4w^2},$$
$$\text{and} \quad l_p \equiv \beta\kappa,$$

where $\beta = (k_B T)^{-1}$, L is the chain length, and $R(s)$ is the chain radius at s. For example, the oligo(p-phenylenevinylene)-derivative OPV-4 in dodecane has $l_p = 150$ nm at 300 K, a molecule separation $\sigma = 0.35$ nm, and a bonding energy 56 kJ/mol [6] yielding $w \approx 0.2$.

We study M patchy particles in a periodically repeated simulation box of volume V at temperature T by Monte Carlo simulations. The system is equilibrated by performing moves and rotations of single molecules and of whole chains as well as reptation moves. We can simulate a limited temperature range ($k_B T \gtrsim 0.04\epsilon$) as at lower temperatures the probability of removing a molecule from a chain by a simple Monte Carlo move vanishes. We choose to consider molecules bonded if their interaction $V < -0.3\epsilon$. Contrary to the square-well patch potential [2], the potential of Eq. (1) makes the average energy per bond E_{bond} temperature dependent. We find that equipartition (i.e., $E_{\text{bond}} = -\epsilon + 3k_B T$, independent of w) applies up to $k_B T \lesssim 0.07\epsilon$, where $E_{\text{bond}} \approx -0.79\epsilon$.

Supramolecular polymerization is reversible, and there exists an equilibrium density ρ_N of chains with length N, with $N = 1, 2, \ldots, \infty$. The total density is given by $\rho = \sum_{N=1}^{\infty} N\rho_N$. The average chain length $\bar{N}$, the aggregation fraction η [9], and the fraction of unbonded sites X [2] are defined as

$$\bar{N} \equiv \frac{\sum_{N=1}^{\infty} N\rho_N}{\sum_{N=1}^{\infty} \rho_N} = \frac{1}{X}, \quad \eta \equiv \frac{\sum_{N=2}^{\infty} N\rho_N}{\sum_{N=1}^{\infty} N\rho_N} = 1 - \frac{1}{\bar{N}^2}. \quad (2)$$

In the ideal free-association (IFA) model [9] each bond has energy ϵ and the polymers form an ideal gas so that $\rho_N \sim \rho_1^N$

$$\bar{N} = \frac{1}{2} + \frac{1}{2}\sqrt{1 + 8\rho\Delta}, \quad \text{with} \quad \Delta = \frac{\upsilon}{2}\exp(\beta G), \quad (3)$$

where $G \lesssim \epsilon$ is an effective free energy per bond and υ is the available bonding volume per particle. Both parameters

are not known *a priori* and are usually fit to the average chain lengths, determined by, e.g., circular dichroism measurements [6]. The WTPT includes the spatial extension of the molecules [10] neglected in the IFA model, by calculating a reference hard-sphere free energy and adding the attractive contribution of the pair potential $V_{\text{att}}(r)$. WTPT also assumes that only one interaction per attractive site is possible. The average chain length predicted by the WTPT is given by Eq. (3), with $\Delta = \Delta^W$

$$\Delta^W \equiv 4\pi \int g_{\text{rep}}(r)\langle\exp(-\beta V_{\text{att}}(r)) - 1\rangle_{\omega_1, \omega_2} r^2 dr, \quad (4)$$

where Δ^W involves a single site-site interaction and is related to the second virial coefficient [2], $\langle.\rangle_{\omega_1, \omega_2}$ denotes an average over all orientations ω_1 and ω_2 of the two molecules, and $g_{\text{rep}}(r)$ is the pair correlation function of the hard-sphere part of the potential. At low densities and temperatures the IFA model and the WTPT are equivalent, and for square-well patchy particles, G becomes the well depth and υ is calculated analytically [2].

In Fig. 2 we compare the aggregation fraction η as a function of temperature T for several values of the flexibility w to the prediction of the WTPT with $g_{\text{rep}}(r) = 1$, appropriate at low densities, and Δ^W [Eq. (5)] numerically calculated. The remarkable agreement with simulations shows that the WTPT also holds for smoothly varying potentials on a hard sphere. We also show a fit of the IFA model that deviates at higher temperatures due to the temperature dependence of the association energy. We find (not shown) that this deviation reduces with decreas-
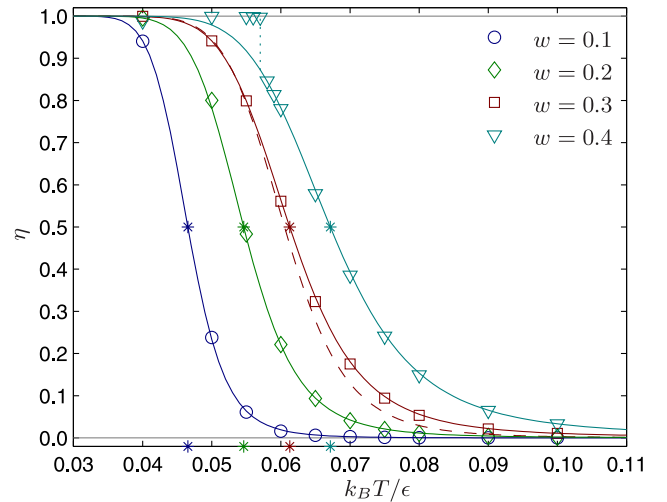

FIG. 2 (color online). Temperature dependence of the aggregation fraction η [Eq. (2)] for several values of the flexibility w for $M = 1330$, $\rho = 1.13 \times 10^{-3}\sigma^{-3}$. $\eta = 1/2$ defines the polymerization temperature T^*, indicated by an asterisk on the curves and on the horizontal axis. At $w = 0.4$ a transition from a gas of chains to a solid bundle at $k_B T = 0.057\epsilon$ is indicated by the dotted line. Symbols denote simulation results, and solid lines are the WTPT. The dashed line is a fit of the IFA model to the curve of $w = 0.3$, with $\upsilon = 1.4 \times 10^{-4}\sigma^3$ and $G = 0.91\epsilon$.

ing w and is negligible for $w < 0.1$. The polymerization temperature T^* is defined as the temperature where half of the molecules has aggregated, i.e., where $\eta(T^*) = \frac{1}{2}$. T^* increases with w due to an increase in available bonding volume v, or, equivalently, because a transition from an unbound to a bound state costs less entropy for a more flexible chain. For $w = 0.4$ and $k_B T < 0.058\epsilon$ a sudden jump to $\eta \approx 1$ occurs. The chains have bundled, with a concomitant increase of the average chain length and a strong depletion of the gas density. Such a sudden increase of η, not accounted for by polymerization theory, has recently been observed for the OPV-4 molecule [6].

By analyzing the radial distribution function and visual inspection, we find the bundles to have an approximate fcc structure with the bundle long axis along the 110. The crystal is not exactly fcc because it is slightly elongated along the bundle axis and contains defects. We also observe that the bundle diameter increases with density, which makes it unlikely that this patchy-particle model describes bundles of fixed finite thickness. However, we observe that thick bundles with a perfect crystal structure evolve towards prolate ellipsoids, with a much smaller aspect ratio than found growing from a polymer gas in our simulations. We believe that the long bundles we observe correspond to metastable structures resulting from kinetic growth pathways that prefer formation of long bundles, since sideways growth is only possible by a surface nucleation event or the association of polymer chains. The latter are increasingly rare, primarily due to the finite number of particles in the simulation box. The equilibrium crystal shape might be reached faster, e.g., by simulating in the grand canonical ensemble and/or by using smart Monte Carlo moves. However, the observed metastable structures might become the true equilibrium structure in the presence of chirality or larger strain in the model, as proposed in Ref. [11].

Now we examine the bundling transition in more detail. Figures 3(a) and 3(b) show the dramatic difference between a bundled and a polymer gas configuration, while the temperatures differ by only $k_B \Delta T = 0.01\epsilon$. In the bundle the individual chains remain identifiable, with no connections between chains. Visual inspection of the process of bundling shows that when three chains come together, they remain bonded and suddenly grow in length, suggesting a nucleation mechanism. In Fig. 3(c), the bundling transition is visible as a sharp jump of the average chain length $\bar{N}(T)$. The dashed line represents systems heated up from a bundled configuration at $k_B T = 0.057\epsilon$. This hysteresis, together with the nucleation mechanism, is evidence for a first-order phase transition. We identify the bundling temperature T_b at the high end of the hysteresis loop, at $k_B T_b \approx 0.065\epsilon$. In the inset of Fig. 3(c) we show $\bar{N}(T)$ for several values of w. Although a stiffer chain loses less entropy upon bundling than a flexible one, T_b increases with flexibility w, similar to T^*. The transition is thus not driven by entropy, but by the interaction energy of neigh-
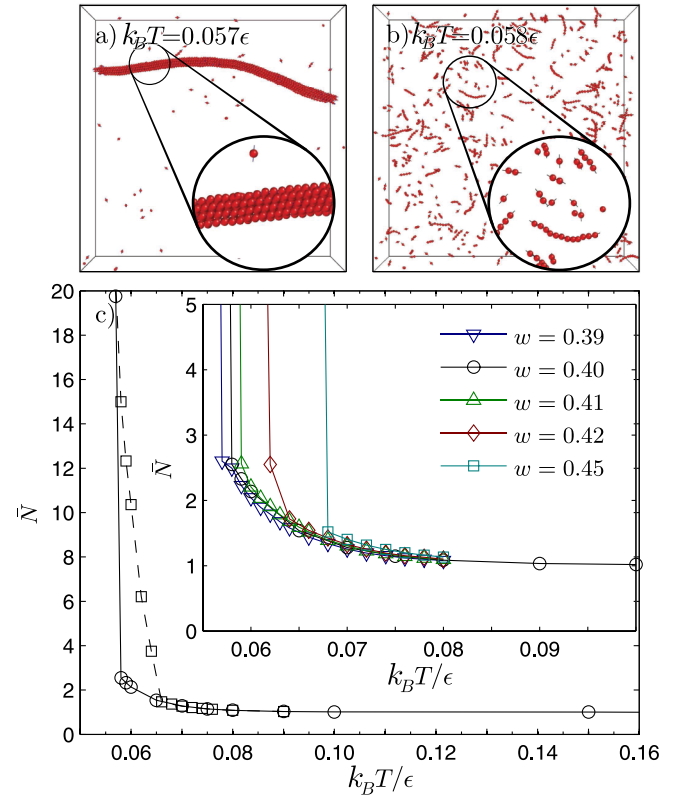

FIG. 3 (color online). Top: Representative configuration for $w = 0.4$ at two very close temperatures. M, ρ as in Fig. 2. (a) $k_B T = 0.057\epsilon$, where a solid bundle has nucleated. (b) $k_B T = 0.058\epsilon$, where the system is still a polymer gas. (c) Average chain length $\bar{N}(T)$ for $w = 0.4$. The solid line shows the jump of $\bar{N}$ for $k_B T \approx 0.057\epsilon$ on cooling. The dashed line shows the hysteresis while raising T from an equilibrated system initially at $k_B T = 0.057\epsilon$. Inset: Same curve for several values of w. No hysteresis loop is shown. Notice that the bundling temperature increases with w.

boring chains [Eq. (1)] that, at large θ, increases with w. Assuming the patches in neighboring chains to be perfectly aligned, the smallest angle θ_i between molecules in neighboring chains is $\theta_i \sim \arctan(2^{-1/6}) \approx 0.73$ rad or $42°$. For $w \lesssim 0.15$ this lateral interaction is negligible ($\theta_i / 2w \approx 2.4$). Increasing w also increases the available lateral bonding volume, decreasing the entropy loss upon bundling.

We interpret the bundling as a sublimation transition, from a polymer gas to a solid bundle. To derive an approximate equation of state, we equate the chemical potential μ_{sol} of a bundle to that of a polymer gas μ^p. By using the IFA model, we can derive

$$\mu^p = \frac{\partial F}{\partial M} = \mu^m - \frac{2}{\beta} \ln\bar{N}, \quad \text{with} \quad \mu^m = \frac{1}{\beta} \ln\left[\frac{v\rho}{Z_1}\right],$$
(5)

where μ^m is the chemical potential of an ideal gas of monomers with internal partition function Z_1, and where $\bar{N}$ is given either by the IFA model [Eq. (3)] or by the WTPT [Eqs. (3) and (4)]. For our rigid molecules, $Z_1 = 1$.

We then model the bundle by an Einstein crystal [12] with

$$\mu_{\text{sol}} = -\epsilon_{\text{sol}} + \frac{1}{\beta} \ln\left[\Lambda^3 \left(\frac{\beta k}{2\pi}\right)^{3/2} \right], \quad (6)$$

where ϵ_{sol} and k are the equilibrium energy and the spring constant of the Einstein crystal, respectively. We replace the de Broglie wavelength term with the bonding volume $\Lambda^3 = \upsilon$, as was done to derive the IFA model. Equating μ^m of Eq. (5) to μ_{sol} of Eq. (6) results in the sublimation line of an ideal gas of monomers ρ_{sub}^m

$$\rho_{\text{sub}}^m = \left(\frac{\beta k}{2\pi}\right)^{3/2} \exp(-\beta\epsilon_{\text{sol}}). \quad (7)$$

Solving $\mu^p = \mu_{\text{sol}}$ yields the sublimation density for the polymer gas ρ_{sub}^p

$$\rho_{\text{sub}}^p = \frac{\rho_{\text{sub}}^m}{(2\rho_{\text{sub}}^m \Delta - 1)^2}. \quad (8)$$

It is useful to define the density at the polymerization temperature $\rho^* = \rho(T^*)$, by combining Eqs. (2) and (3)

$$\eta(T^*) = \frac{1}{2} \Rightarrow \rho^* = \frac{2 - \sqrt{2}}{2\Delta}. \quad (9)$$

Comparison of ρ_{sub}^p to ρ^* allows us to estimate whether the sublimation transition is dominated by the bundling of polymers [Eq. (8)] or of monomers [Eq. (7)].

In Fig. 4, we compare the $T - \rho$ phase diagram resulting from our simulations to the theoretical polymerization and sublimation line. The parameters of the Einstein crystal were determined by fitting Eq. (8) to our simulations, with $\Delta = \Delta^W$ of Eq. (4), and the polymerization density ρ^* calculated from the WTPT. At low densities $\rho_{\text{sub}}^p \sim \rho_{\text{sub}}^m$,

since the polymerization temperature is lower than the sublimation temperature, i.e., $T^* < T_b$. The sublimation lines differ at higher densities because μ^p tends to a finite value, whereas the chemical potential of an ideal monomer gas tends to zero. The average polymer length $\bar{N}$ at the sublimation transition increases for decreasing w. When the lateral interactions vanish ($w < 0.15$), the bundling transition would occur for infinitely long polymers. The agreement between ρ_{sub}^p and our simulations suggests that this approximate theory describes the essential physics of our patchy-particle model.

In summary, we have presented a patchy-particle model that describes supramolecular polymerization and displays a first-order phase transition to bundles due to weak chain-chain interactions. The chain-to-bundle transition can be seen as a sublimation transition from a polymer gas to a solid bundle, for which we have given a qualitative equation of state. We have related the occurrence of the phase transition to the polymer flexibility. Our simulations show that bundling leads to a sudden increase of the average length of the aggregates. From the simulations, it is unlikely that these simple patchy particles can describe fibers with an intrinsically limited thickness. However, we believe that the patchy particle is a powerful tool for efficient modeling of complex, self-assembling systems that can be improved by including more specific, e.g., chiral, chain-chain interactions, which might lead to bundles with fixed finite thickness.
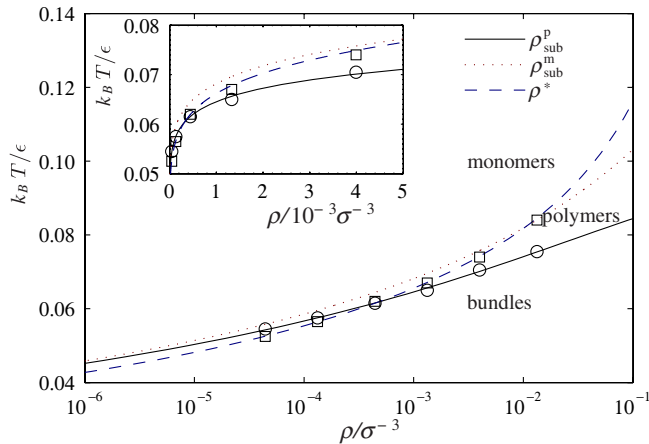
FIG. 4 (color online). Simulated gas-solid coexistence line (circles) and polymerization line (squares) for $w = 0.4$, together with the theoretical monomer sublimation line ρ_{sub}^m [Eq. (7), dotted line], polymer sublimation line ρ_{sub}^p [Eq. (8), solid line], and polymerization line ρ^* [Eq. (9), dashed line] based on the WTPT description of a polymer gas in equilibrium with an Einstein crystal, with $k = 1.2 \times 10^3 \epsilon\sigma^{-2}$ and $\epsilon_{\text{sol}} = 1.05$. In the inset we show the same, but on a linear density scale.

[1] R. F. Service, Science **309**, 95 (2005).
[2] F. Sciortino, E. Bianchi, J. F. Douglas, and P. Tartaglia, J. Chem. Phys. **126**, 194903 (2007).
[3] A. W. Wilber *et al.*, J. Chem. Phys. **127**, 085106 (2007).
[4] Z. Zhang, A. S. Keys, T. Chen, and S. C. Glotzer, Langmuir **21**, 11547 (2005).
[5] H. Engelkamp, S. Middelbeek, and R. J. M. Nolte, Science **284**, 785 (1999).
[6] P. Jonkheijm, P. van der Schoot, A. P. H. J. Schenning, and E. W. Meijer, Science **313**, 80 (2006).
[7] L. Brunsveld *et al.*, Proc. Natl. Acad. Sci. U.S.A. **99**, 4977 (2002).
[8] C. P. Lowe, Phil. Trans. R. Soc. B **358**, 1543 (2003).
[9] P. van der Schoot, in *Theory of Supramolecular Polymerization*, edited by A. Ciferri, Supramolecular Polymers (CRC Press, Boca Raton, FL, 2005), 2nd ed.
[10] M. Wertheim, J. Stat. Phys. **35**, 19 (1984); **35**, 35 (1984); **42**, 459 (1986).
[11] G. M. Grason and R. F. Bruinsma, Phys. Rev. Lett. **99**, 098101 (2007).
[12] D. Frenkel and A. J. C. Ladd, J. Chem. Phys. **81**, 3188 (1984).